

Enhanced superconducting vortex pinning with disordered nanomagnetic arraysY. J. Rosen,^{1,*} A. Sharoni,^{1,2} and Ivan K. Schuller¹¹*Department of Physics, University of California–San Diego, La Jolla, California 92093-0319, USA*²*Department of Physics, Bar Ilan University, Ramat Gan 52900, Israel*

(Received 25 February 2010; revised manuscript received 8 June 2010; published 9 July 2010)

We studied the effect of disorder on superconducting vortex pinning produced by arrays of artificial pinning sites. The magnetoresistance of samples with pinning configurations varying from a triangular array to an almost random distribution of pinning sites provides a controlled system for such studies. Interestingly even small degrees of order are sufficient to produce enhanced pinning at well-defined magnetic fields. These effects increase with increasing order and evolve toward the expected matching minima for a triangular array. Surprisingly, the position of the first matching minimum decreases with increasing disorder. Furthermore, additional matching minima appear at higher field values which do not coincide with commonly observed triangular pinning lattice matching minima.

DOI: [10.1103/PhysRevB.82.014509](https://doi.org/10.1103/PhysRevB.82.014509)

PACS number(s): 74.25.Wx, 74.62.En, 47.32.cb

I. INTRODUCTION

Vortex pinning in superconductors with artificially produced pinning arrays provide an ideal controllable model system for a periodic system moving in the presence of a periodic potential. Such physical systems appear also in studies of the interaction between epitaxial films,¹ confined charged plasmas,² biological ratchets,³ etc. Moreover a number of new phenomena have been engineered into superconducting systems such as field-driven superconductivity,⁴ bistability,⁵ ratchet effects,⁶ and new Josephson effects.⁷ Additionally, this type of pinning may provide the means for enhancing critical current densities for superconducting transmission lines^{8,9} and reducing noise in a variety of superconductivity based devices.¹⁰

Modern nanolithography enables positioning pinning structures at length scales similar to the vortex interaction length in superconductors. This provides the means to manipulate the potential-energy landscape. For instance, square or triangular pinning arrays produce substantial increases in the critical current for magnetic fields corresponding to an integer ratio between the density of vortices and of the pinning sites.¹¹ This effect is pronounced in transport measurements where the resistance decreases by several orders of magnitude at specific magnetic fields.¹² These are known as the matching minima. Rectangular,^{13,14} kagome,¹⁵ honeycomb,¹⁶ and quasiperiodic arrays such as the Penrose lattice,^{17,18} Fibonacci series, and fractal structures¹⁹ show more complex matching minima structures due to the interplay between the array symmetries and the vortex lattice. These have been extensively studied.²⁰

The role of disorder and defects in a lattice, although of much importance in condensed-matter physics, has received little attention in this context. The extreme case of intrinsic defects lacking any order has been studied for both high and low T_c superconductors.^{21–24} These defects, which act as pinning sites, while causing an increase in the critical current, show no matching minima or commensuration effects.¹⁷ The importance of lattice imperfections was recently demonstrated for a triangular pinning lattice with vacancies.^{25,26} In this case, the lattice symmetry and the density of the lattice

sites compete for the commensurate vortex lattice matching minima. There are few additional studies which measure the effects of only a particular type of order, with either short-range order²⁷ of several lattice sites or long-range order.^{28–30} Both report the presence of matching minima but do not provide a quantitative comparison with other disordered and ordered lattices. Thus, a comprehensive study where the type and amount of disorder is systematically controlled is needed.

II. EXPERIMENTAL

In this paper we report on matching minima of superconducting vortices in artificial pinning arrays with controlled short-range order. The pinning-site configuration was varied from an ordered triangular lattice to a nearly random array. We find enhanced periodic matching even for the most disordered array. When the disorder increases the matching minima become less pronounced. Interestingly, the centers of the first matching minima shift toward lower fields as a function of increasing disorder.

We use the two-dimensional “car parking” algorithm to generate pinning configurations with controlled degrees of short-range order.³¹ The most ordered realization of the algorithm resembles a two-dimensional closed-packed triangular lattice. An order parameter in the algorithm allows control of the short-range order. When this order parameter approaches zero, the configuration tends toward a random one. The minimum distance between pinning sites, D , acts as such an order parameter. To generate the structure the pinning sites are positioned randomly and sequentially in a $67 \times 67 \mu\text{m}^2$ area. As the array is generated, the distance between a newly assigned site and its nearest neighbor is measured to determine if it is larger than D . If it is not, the site is erased and a new position assigned to it. This process is continued until all 23 000 pinning sites are assigned so that for all structures the average density is equal to that of a triangular lattice with a lattice constant of 480 nm.

The samples were fabricated on Si substrates using a conventional lift-off technique combined with sputtering. The pinning sites were written in polymethyl methacrylate using

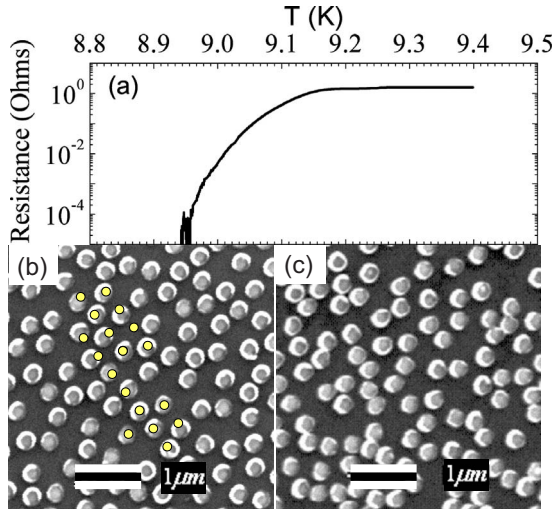


FIG. 1. (Color online) (a) R vs T curve for sample $D = 225$ nm at 2 kA/cm². Below: 4×4 μm^2 SEM images of the (b) $D = 370$ nm and (c) $D = 280$ nm samples, respectively. Small (yellow) circles in (b) are a guide to the eyes showing an area where the pinning sites have triangular lattice symmetry.

standard e-beam lithography. Cobalt dots (250 nm diameter and 40 nm thick) were prepared using standard ac sputtering and liftoff. To complete the structure, a 100 nm layer of Nb was evaporated on top of the dots, and then photolithographically patterned to a 50×50 μm^2 resistance bridge. Magnetoresistance measurements were conducted in a variable temperature liquid-He flow cryostat with temperature stability better than 1 mK. The resistance was measured using a current source and nanovoltmeter in standard dc polarity reversal mode.³² Each sample was measured at four different temperatures ranging from $T/T_c = 0.96$ to 0.99. For each temperature several different R vs H curves were obtained with current densities between 0.2–20 kA/cm². Typically the Nb had a T_c of 9.0 K and a transition width of 0.2 K [Fig. 1(a)]. T_c is defined as the temperature at which the resistance is equal to 90% of the normal resistance.

Five samples (see Table I) with different degrees of disorder were investigated. For comparison we measured a sample with a regular triangular array and a lattice spacing of 480 nm. The other four have increasing degrees of disorder, generated using $D = 370, 335, 280,$ and 225 nm, all with the

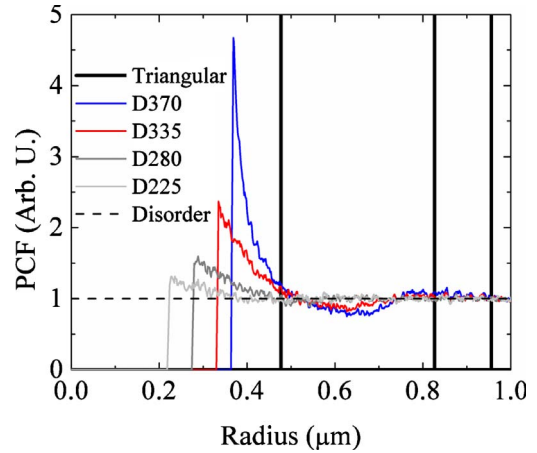


FIG. 2. (Color online) The PCF for the different samples arranged from the most ordered (top, blue) to the most disordered (bottom, light gray). The dashed horizontal line denotes the PCF for a disorder system. The radius at which the PCF of a sample decays to this line is the sample's RLO. The vertical thick black lines denote the PCF for the triangular lattice (a series of delta function peaks).

same average density as the triangular lattice. $D = 370$ nm is the most ordered realization the algorithm can produce for this density³³ and for $D = 225$ nm the Co pinning centers start to overlap. In the micrograph of sample $D = 370$ nm [Fig. 1(b)] areas with a relatively ordered triangular lattice are evident. On the other hand, the sample $D = 280$ nm shows no particular order [Fig. 1(c)].

To quantify the degree of disorder in an array, a standard normalized pair-correlation function (PCF) (Ref. 34) was used. The range of local order (RLO) is defined as the distance beyond which the PCF becomes equal to one.³⁴ The PCFs of all samples are shown in Fig. 2, and the corresponding RLOs are summarized in Table I. For the most ordered $D = 370$ nm sample, the PCF oscillates before decaying to unity with an RLO of 1.12 μm . This is slightly longer than the third-nearest-neighbor distance of the triangular lattice. The most disordered $D = 225$ nm sample, has an RLO of 0.41 μm , which is less than the first-nearest-neighbor distance for a triangular or square lattice with the same density.

TABLE I. Sample parameters: minimum distance used to generate disorder, the corresponding RLO and average position of the first matching minimum in units of B_1 . The RLO of an ordered infinite lattice is infinite (Inf). The error of the matching minimum's position is the standard deviation from the eight magnetoresistance curves performed for each measurement.

Sample No.	Minimum distance (nm)	RLO (μm)	Center of first matching minimum (B/B_1)
Triangle	480 ± 5	Inf	1.01 ± 0.02
$D = 370$ nm	370 ± 5	1.12 ± 0.01	1.02 ± 0.03
$D = 335$ nm	335 ± 5	0.95 ± 0.01	0.93 ± 0.02
$D = 280$ nm	280 ± 5	0.63 ± 0.01	0.86 ± 0.02
$D = 225$ nm	225 ± 5	0.41 ± 0.01	0.80 ± 0.06

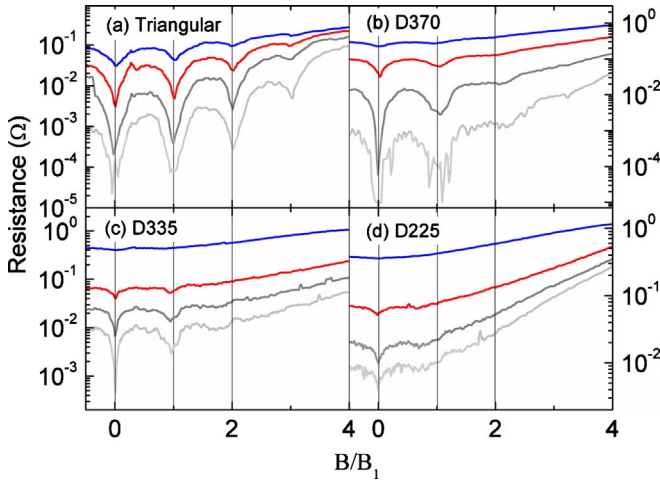


FIG. 3. (Color online) Magnetoresistance (log scale) as a function of field for the different samples. (a) Triangular lattice and (c) $D=335$ nm samples at a constant current density of $I=2.0$ kA/cm². The triangular lattice has $T/T_c=.995, .994, .993,$ and $.992$, and $D=335$ nm has $T/T_c=.987, .983, .980,$ and $.978$. The different T_c 's were chosen because the disordered samples have a transition width about double that of the triangular lattice. (b) Sample $D=370$ nm, the least disordered sample, at constant $T/T_c=.973$ with currents $I=2.0-14$ kA/cm². (d) Sample $D=225$ nm, the most disordered sample, at a constant $T/T_c=.972$ with currents $I=1.4-20$ kA/cm². There is no change in the matching minima positions as a function of either temperature or current.

III. RESULTS AND DISCUSSION

Figures 3(a)–3(d) shows the magnetoresistance of samples with different degrees of disorder at currents and temperatures which display the most pronounced matching minima for each sample. The magnetic field was normalized to the first integer matching minimum of the triangular lattice, $B_1=\beta\phi_0$, where $\phi_0=20.7$ G μm^2 is the flux quantum and β is the pinning-site density.^{11,35} Vertical lines at integer matching minima are added as a guide to the eyes. The magnetoresistance minima indicate matching effects between the vortex lattice and the pinning sites.¹² The locations of match-

ing minima are not affected by temperature [Figs. 3(a) and 3(c)] or current [Figs. 3(b) and 3(d)] in any of the samples. The superconducting transition widths of the disordered samples were about double that of the triangular sample. It is therefore difficult to compare the triangular sample to disordered samples at similar values of T/T_c 's.

The matching minima of the triangle pinning-site lattice are shown in Fig. 3(a) for different temperatures and a current density of 2 kA/cm². Three matching minima appear at the expected magnetic fields as predicted by the pinning-site density. The magnetoresistance of sample $D=370$ nm [Fig. 3(b)] also exhibits a first matching minima as expected from the pinning-site density. However, the high-field features are different from those of the triangular lattice, in spite of the fact that this is the least disordered sample. The second matching minimum is barely observable, *not* located at an integer multiple of B_1 , and there is no discernible third matching minimum. With increasing disorder [Figs. 3(c) and 3(d)] the matching minima become wider and shallower. However, matching minima appear even for the most disordered sample ($D=225$ nm). To emphasize the less pronounced features we show in Fig. 4(a) representative magnetoresistance curves for each sample, in which the background resistance was subtracted. Matching minima can be resolved for all samples for all degrees of disorder. For example, even sample $D=225$ nm (most disordered, top light gray curve) shows a wide minimum centered around $0.8B_1$.

Surprisingly, with increasing pinning-site disorder the first minimum shifts toward lower fields. Figure 4(b) shows the positions of the first matching minima averaged over eight measurements versus the RLO. The first matching minimum increases in field linearly with the RLO and reaches the value of the triangular lattice (dashed line) at $D=370$ nm. For all disordered samples there are additional magnetoresistance features at higher fields [see Fig. 4(a)]. These appear as smaller peaks and valleys with their position changing from sample to sample, indicating complex sample-specific matching effects. For example, in sample $D=280$ nm [dark gray curve, second from the top in Fig. 4(a)] there is one matching minimum at slightly less than B_1 , and two small minima at $B/B_1=1.6$ and 2.5 . The first matching minimum is

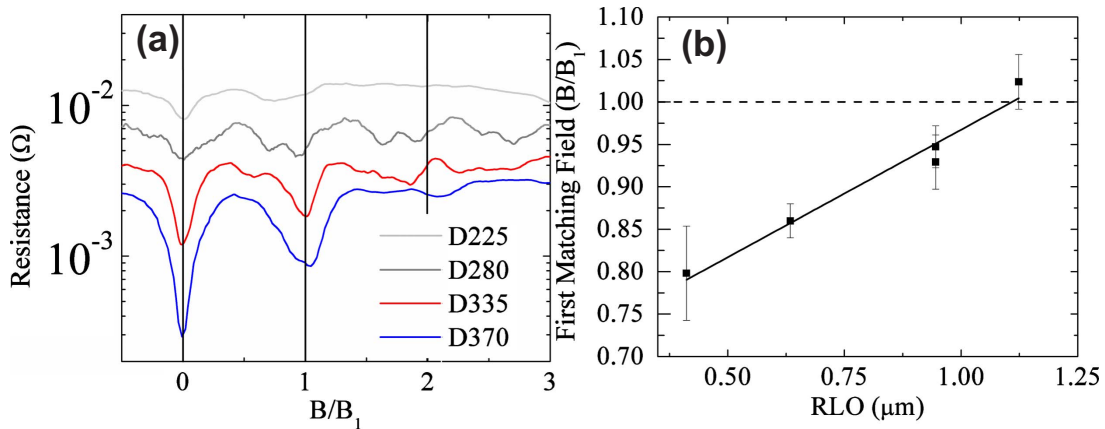


FIG. 4. (Color online) (a) Magnetoresistance as a function of field for different samples with backgrounds subtracted and heights shifted for clarity. The measurements were done at $T/T_c=0.97-0.98$ and at currents of 1.4–2.0 kA/cm². (b) The position of the first matching minimum for different samples plotted against the RLO. The dotted line is the theoretical first minimum position of a triangular lattice.

in the vicinity of the expected magnetic field, but the additional features have no relation to other expected matching minima. These features were reproduced at different temperatures and currents, ruling out experimental artifacts.

While measurements of systems without ordered pinning centers do not show matching related minima and enhanced vortex pinning,¹⁷ we find that the smallest order in the pinning potential leads to matching minima. This remains true even for the most disordered sample, where the PCF is almost flat and the RLO is shorter than the lattice constant of a triangular array with the same pinning density. Our results indicate that there is critical matching between the vortex lattice and the magnetic dots, and it originates at a local length scale. In other words, there are local pinning-site configurations that repeat with similar parameters (of density and symmetry) throughout the sample that allow enhanced vortex pinning at particular fields. These configurations have a low number of pinning centers associated with them and are scattered about the sample in random locations and orientations as is consistent with a disordered sample.

This scenario is in agreement with experiments on quasiperiodic Fibonacci pinning arrays and disordered systems.^{19,36} Here too, the local matching yields shallow minima. This is due to the fact that matching occurs in many different locations but only on a small percentage of the sample. Thus, our results indicate that any amount of order shown as a nonunity PCF implies there are areas with local order that enhance the vortex lattice pinning at particular fields. Accordingly, one would expect the matching minima to occur at vortex densities related to the length scale for which the PCF has a maximum. The distance of the PCF maximum decreases with increasing disorder (Fig. 2). This should result in the matching minima appearing at larger fields for increasingly disordered samples. Surprisingly, our results [see Fig. 4(a)] indicate the opposite. Increasing the disorder leads to smaller fields for the first matching minima. Thus, the ordered structures responsible for matching of the vortex lattice in our films are of lower density and do not relate to the PCF peak. Interestingly, we find a linear correlation of the RLO with the first matching minima positions [see Fig. 4(b)]. A lower RLO means there is less long-range order. The vortex lattice, which energetically prefers long-range order, must deform in order to pin to the pinning sites. This causes the vortices to be in a less stable pinning configuration and more susceptible to flux creep, which may explain why the matching minima become shallow. One can account for the magnetoresistance minima shifting to a lower field in the following way. At all distances shorter than the RLO the pinning sites contain a certain degree of order. The vortex-vortex interaction is repulsive (decaying approximately exponentially as a function of R/λ ,³⁷ where R is the vortex-vortex distance and λ is the magnetic field penetration depth). This means that at lower vortex densities, and therefore larger average vortex-vortex distances, the force on each

vortex is smaller, allowing it to relax and pin better to the disordered pinning lattice. Thus, the best vortex lattice pinning (the minima in the magnetoresistance) will occur at the lowest vortex density for which there still is long-range order, and this is the RLO.

The high-field landscape of the magnetoresistance is very interesting and different from that found in disordered, quasiperiodic, or vacancy potentials.²⁵ For quasiperiodic potential since only a fraction of the vortices are pinned, at higher fields the elastic energy is large and overcomes the pinning.¹⁹ In triangular lattice with vacancies there were no indications of complex high-field vortex lattice pinning.²⁵ We find that at higher fields there are additional shallow minima that do not relate to higher order “main” pinning potentials. These features change from sample to sample but are reproducible in each sample for all temperatures and current densities. In this case the combination of partial order in a disordered media may help the vortex lattice pin to complex interstitial vortex configurations, which are related to the specific order-disorder realization.

IV. CONCLUSIONS

In summary, we measured superconducting vortex pinning in a disordered pinning potential with controlled short-range order generated using the car parking algorithm. Magnetoresistance minima characteristic of matching effects are observed even for the smallest degree of order. This indicates that even very low pinning-site symmetry is sufficient for enhanced pinning of the vortex lattice at specific matching fields. The most ordered potential generated by the car parking algorithm shows a pronounced first matching minimum corresponding to the matching minima of a triangular lattice with the same pinning-site density. Increasing the disorder results in the first matching minimum becoming less pronounced, as may be expected, but also in it shifting to lower fields.

We report on the appearance of additional magnetoresistance features at higher fields. These are reproducible for all temperatures and current densities measured, but vary from sample to sample. We attributed these matching minima to complex interstitial vortex pinning arising from the short-range order generated by the algorithm.

Further theoretical and numerical analyses are needed to quantitatively understand these phenomena, and we hope that our study will motivate research of vortex dynamics theories in this direction. These must account for the fact that small amounts of order in the pinning sites lead to enhanced pinning at fields lower than the matching fields due to the reduced range of local order.

ACKNOWLEDGMENTS

We thank Y. Bruynseraede, J. L. Vicent, D. Perez-Lara, E. Gonzalez, and J. Villegas for useful conversations. This work has been supported by the National Science Foundation.

*Corresponding author; yrosen@ucsd.edu

- ¹A. Catana, J. P. Locquet, S. M. Paik, and I. K. Schuller, *Phys. Rev. B* **46**, 15477 (1992).
- ²C. F. Driscoll, D. Z. Jin, D. A. Schechter, and D. H. E. Dubin, *Physica C* **369**, 21 (2002).
- ³R. D. Astumian, *Science* **276**, 917 (1997).
- ⁴M. Lange, M. J. Van Bael, Y. Bruynseraede, and V. V. Moshchalkov, *Phys. Rev. Lett.* **90**, 197006 (2003).
- ⁵J. E. Villegas, C. P. Li, and I. K. Schuller, *Phys. Rev. Lett.* **99**, 227001 (2007).
- ⁶J. E. Villegas, S. Savel'ev, F. Nori, E. M. Gonzalez, J. V. Anguita, R. Garcia, and J. L. Vicent, *Science* **302**, 1188 (2003).
- ⁷A. Gilabert, I. K. Schuller, V. V. Moshchalkov, and Y. Bruynseraede, *Appl. Phys. Lett.* **64**, 2885 (1994).
- ⁸L. Civale, A. D. Marwick, T. K. Worthington, M. A. Kirk, J. R. Thompson, L. Krusin-Elbaum, Y. Sun, J. R. Clem, and F. Holtzberg, *Phys. Rev. Lett.* **67**, 648 (1991).
- ⁹E. H. Brandt, *Rep. Prog. Phys.* **58**, 1465 (1995).
- ¹⁰P. Selders and R. Wordenweber, *Appl. Phys. Lett.* **76**, 3277 (2000).
- ¹¹Y. Jaccard, J. I. Martín, M. C. Cyrille, M. Vélez, J. L. Vicent, and I. K. Schuller, *Phys. Rev. B* **58**, 8232 (1998).
- ¹²J. I. Martín, M. Vélez, J. Nogués, and I. K. Schuller, *Phys. Rev. Lett.* **79**, 1929 (1997).
- ¹³J. I. Martín, M. Vélez, A. Hoffmann, I. K. Schuller, and J. L. Vicent, *Phys. Rev. B* **62**, 9110 (2000).
- ¹⁴J. E. Villegas, E. M. González, M. I. Montero, I. K. Schuller, and J. L. Vicent, *J. Phys. Chem. Solids* **67**, 482 (2006).
- ¹⁵D. J. Morgan and J. B. Ketterson, *Phys. Rev. Lett.* **80**, 3614 (1998).
- ¹⁶T. C. Wu, J. C. Wang, L. Horng, J. C. Wu, and T. J. Yang, *J. Appl. Phys.* **97**, 10B102 (2005).
- ¹⁷M. Kemmler, C. Gurlich, A. Sterck, H. Pohler, M. Neuhaus, M. Siegel, R. Kleiner, and D. Koelle, *Phys. Rev. Lett.* **97**, 147003 (2006).
- ¹⁸R. B. G. Kramer, A. V. Silhanek, J. Van de Vondel, B. Raes, and V. V. Moshchalkov, *Phys. Rev. Lett.* **103**, 067007 (2009).
- ¹⁹J. E. Villegas, M. I. Montero, C. P. Li, and I. K. Schuller, *Phys. Rev. Lett.* **97**, 027002 (2006).
- ²⁰M. Vélez, J. I. Martín, J. E. Villegas, A. Hoffmann, E. M. González, J. L. Vicent, and I. K. Schuller, *J. Magn. Magn. Mater.* **320**, 2547 (2008).
- ²¹T. Giamarchi and P. Le Doussal, *Phys. Rev. Lett.* **76**, 3408 (1996).
- ²²D. S. Fisher, M. P. A. Fisher, and D. A. Huse, *Phys. Rev. B* **43**, 130 (1991).
- ²³B. Rosenstein and V. Zhuravlev, *Phys. Rev. B* **76**, 014507 (2007).
- ²⁴G. Blatter, M. V. Feigel'man, V. B. Geshkenbein, A. I. Larkin, and V. M. Vinokur, *Rev. Mod. Phys.* **66**, 1125 (1994).
- ²⁵M. Kemmler, D. Bothner, K. Ilin, M. Siegel, R. Kleiner, and D. Koelle, *Phys. Rev. B* **79**, 184509 (2009).
- ²⁶C. Reichhardt and C. J. Olson Reichhardt, *Phys. Rev. B* **76**, 094512 (2007).
- ²⁷J. Eisenmenger, M. Oettinger, C. Pfahler, A. Plettl, P. Walther, and P. Ziemann, *Phys. Rev. B* **75**, 144514 (2007).
- ²⁸D. M. Silevitch, D. H. Reich, C. L. Chien, S. B. Field, and H. Shtrikman, *J. Appl. Phys.* **89**, 7478 (2001).
- ²⁹X. Hallet, M. Matefi-Tempfli, S. Michotte, L. Piraux, J. Vanacken, V. V. Moshchalkov, and S. Matefi-Tempfli, *Small* **5**, 2413 (2009).
- ³⁰C. Reichhardt, J. Groth, C. J. Olson, S. B. Field, and F. Nori, *Phys. Rev. B* **54**, 16108 (1996).
- ³¹H. Solomon, *Proceedings of the Fifth Berkeley Symposia on Mathematical Statistics and Probability*, Vol. III: Physical Sciences (University of California Press, Berkeley, California, 1967), p. 119.
- ³²A. Daire, W. Goeke, and M. A. Tupta, White Paper: New Instruments Can Lock Out Lock-ins, Keithley Instruments, Inc., Cleveland, OH, 2005.
- ³³J. Feder, *J. Theor. Biol.* **87**, 237 (1980).
- ³⁴J. M. Ziman, *Models of Disorder: The Theoretical Physics of Homogeneously Disordered Systems* (Cambridge University Press, Cambridge, New York, 1979).
- ³⁵A. T. Fiory, A. F. Hebard, and S. Somekh, *Appl. Phys. Lett.* **32**, 73 (1978).
- ³⁶J. E. Villegas, E. M. Gonzalez, Z. Sefrioui, J. Santamaria, and J. L. Vicent, *Phys. Rev. B* **72**, 174512 (2005).
- ³⁷E. H. Brandt, *Phys. Rev. B* **34**, 6514 (1986).